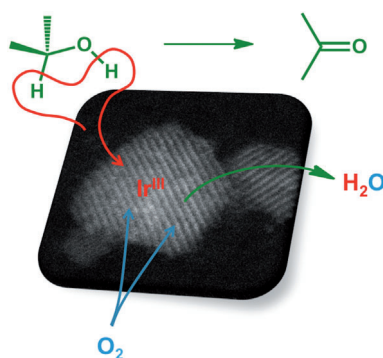


FULL PAPERS

An idea in transit. Iridium oxide, supported on nanoparticulate cerium oxide, is reported to catalyze the oxidative dehydrogenation of alcohols via β -hydride elimination. The catalyst surface can be reoxidized with either a molecular oxygen or a ketone, which completes the transfer hydrogenation cycle.



*C. Hammond, M. T. Schümperli,
S. Conrad, I. Hermans**

■■ - ■■

**Hydrogen Transfer Processes
Mediated by Supported Iridium Oxide
Nanoparticles**



DOI: 10.1002/cctc.201300253

Hydrogen Transfer Processes Mediated by Supported Iridium Oxide Nanoparticles

Ceri Hammond, Martin T. Schümperli, Sabrina Conrad, and Ive Hermans*^[a]

Homogeneous iridium catalysts have demonstrated exceptional catalytic activity for a number of hydrogen transfer reactions. Herein, we demonstrate the synthesis of a heterogeneous iridium catalyst supported on nanoparticulate cerium oxide and investigate its application for the aerobic oxidation of benzyl alcohol and the Meerwein–Ponndorf–Verley transfer hydrogenation of cyclohexanone. Along with the optimisation of the activity of the catalyst, the kinetic parameters have been examined to unravel the elementary reaction steps mediated

by this catalyst and further rationalise the observed structure–activity relationships. Both spectroscopic and catalytic investigations suggest that iridium oxide nanoparticles, most likely Ir₂O₃, mediate these reactions via the formation of metal hydroxide species, which are subsequently reoxidised with either a molecular oxygen or a ketone. In contrast to many other metal- or metal oxide-based catalysts, this catalyst can perform the selective oxidation of alcohols in the absence of a base, at mild temperatures and at a low metal loading.

Introduction

In recent years, considerable attention has been paid to the synthesis and exploration of new catalytic materials or complexes based on late transition metals, such as Au, Pd, Ru and Pt. The interest in these elements often lies in their considerable redox potential, their large number of available oxidation states, and their ability to coordinate and activate a number of important substrates, such as dioxygen, hydrogen, alkanes, alcohols and olefins. Thus, these metals are the crucial species in many well-known homogeneous catalysts and can efficiently catalysed processes such as olefin metathesis (e.g. Ru),^[1] carbon–carbon coupling (e.g. Pd)^[2] and the selective oxidation of methane (e.g. Pt).^[3] In contrast to many of the aforementioned transition metals, the chemistry of Ir has received relatively little attention. This is in spite of its promising activity and selectivity for a number of important chemical transformations: (de)hydrogenations,^[4] alkane activation,^[5] preferential CO oxidation,^[6] and more recently steam reforming,^[7] (electro)catalytic water oxidation,^[8] amongst others.^[9] Furthermore, in contrast to the increasing interest in the synthesis of monometallic^[10] and bimetallic^[11] heterogeneous catalysts based on, for example, Au, Pd, Pt and Ru, few reports describe the synthesis and application of a heterogeneous Ir-based catalyst for selective chemical transformations and even fewer describe the use of a heterogeneous Ir catalyst for liquid phase reactions.

Selective oxidation processes are one of the cornerstones of the chemical industry at all levels of the value chain and play

an important role in the functionalisation of molecules. Despite their pre-eminence, they remain some of the most environmentally problematic transformations on an industrial scale, often because of the nature of the oxidative species: bulky and/or toxic inorganic salts of Cr⁶⁺ and Mn⁷⁺ are highly atom inefficient, and oxidants such as alkyl hydroperoxides or Dess–Martin periodinane co-produce stoichiometric quantities of other organic species.^[12] In the context of sustainable chemistry, developing catalysts that can perform selective oxidation processes with ‘green’ and/or environmentally benign oxidants, such as hydrogen peroxide or dioxygen, is a key challenge for the future.

Many selective oxidation processes proceed via the activation of C–H bonds and the subsequent formation of metal hydride or metal hydroxide species. Such species are often the key species formed in many Ir-catalysed transformations,^[13] and we reasoned that if they could be formed on a heterogeneous catalyst, the catalyst may prove to be a suitable material for the selective oxidative dehydrogenation of alcohols to aldehydes/ketones, a key transformation in synthetic chemistry. Considering these factors, we decided to investigate the potential activity and selectivity of various metal oxide-supported Ir catalysts and evaluate their potential as heterogeneous catalysts for aerobic oxidations.

Results and Discussion

Material synthesis and catalyst evaluation

Given that a number of noble metal and metal oxide nanoparticles have recently shown considerable catalytic activity for the aerobic oxidation of alcohols, we decided that a solid catalyst composed of supported iridium (oxide) nanoparticles could prove to be a suitable material from which to begin our

[a] Dr. C. Hammond, M. T. Schümperli, S. Conrad, Prof. Dr. I. Hermans
Institute for Chemical and Bioengineering
ETH Zurich
Wolfgang-Pauli-Strasse 10, CH-8093 Zurich (Switzerland)
Fax: (+41) 44-633-42-58
E-mail: hermans@chem.ethz.ch

Supporting information for this article is available on the WWW under <http://dx.doi.org/10.1002/cctc.201300253>.

investigations. Our preliminary studies therefore focused on the deposition of Ir, in the form of $\text{H}_2\text{Ir}^{\text{IV}}\text{Cl}_6$, onto various high-surface area metal oxides, which are suitable as catalytic support materials. Although impregnation is not the most suitable technique for the preparation of highly dispersed metal (oxide) nanoparticles, this scalable methodology enabled the rapid screening of a number of metal–support combinations (Table 1). From these preliminary studies, we observed that

Entry	Ir loading ^[b]	Support	Preparation method	Yield ^[c]
1	n.a.	no catalyst	n.a.	0
2	2.5	TiO ₂	impregnation	< 1
3	2.5	MgO	impregnation	< 1
4	2.5	CeO ₂	impregnation	16.8
5	1.5	CeO ₂	deposition–precipitation	21.4
6	0.5	CeO ₂	deposition–precipitation	33.4
7	0	CeO ₂	n.a.	8.4

[a] Reaction conditions: 3 h, 90 °C, 0.2 M benzyl alcohol in toluene, 0.5 mol% metal (substrate/metal = 200); [b] wt% metal; [c] calculated as (moles of benzaldehyde produced/initial moles of benzyl alcohol) × 100. All catalysts were pre-treated in air at 400 °C for 3 h, except entry 6 (200 °C, 3 h, air). For entry 7, an equivalent amount of CeO₂ to that used in entry 6 was used as catalyst.

cerium oxide (CeO₂) was the most suitable support material, with a catalyst comprising 2.5 wt% Ir/CeO₂ selectively ($\geq 98\%$) oxidising benzyl alcohol to benzaldehyde at a rather modest yield of 16.8% in 3 h after calcination at 400 °C for 3 h (entry 4). The unique ability of this catalyst composition to mediate this reaction could be due to a number of factors. Firstly, CeO₂ can activate and oxidise alcohols to a small extent, and examination of the analogous reaction catalysed by an excess of CeO₂ alone revealed that this could contribute around one half of the overall activity of the 2.5 wt% Ir/CeO₂ catalyst. Furthermore, CeO₂ is a well-known oxygen pump that can readily donate its lattice oxygen atoms to oxidation reactions. The reduced metal oxide may subsequently be re-oxidised by O₂, and this facile O₂ transport could lead to significant improvements in the catalytic system. Previous work has demonstrated that CeO₂, and particularly nanoparticulate CeO₂, is one of the most optimal support materials for Au-catalysed alcohol oxidation for this reason.^[14]

After identifying Ir/CeO₂ as the most suitable catalyst composition, we focused our attention on the optimisation of the activity of this catalyst. We first investigated alternative methods of preparation and found that a deposition–precipitation (DP) methodology, through which the cationic metal precursor is deposited onto the support at high pH,^[15] lead to improvements in catalytic activity in comparison to the standard impregnation route (Table 1, entry 5). This increase in activity may tentatively be ascribed to two factors. Firstly, it is well known that a DP methodology typically produces smaller nanoparticles with a narrower particle size distribution in comparison to a standard impregnation route, which may positively affect the

activity of the catalyst.^[16] However, given the inapplicability of TEM for this catalyst composition (see below), it is not possible at this stage to confirm this. Secondly, the additional washing method used for DP may lead to a reduction in the chloride (Cl⁻) concentration of the catalyst. Because Cl⁻ ions facilitate 1) the agglomeration of various metal (oxide) particles^[17] and 2) poison catalytic active sites,^[18] their absence from the DP catalyst in comparison to the impregnated catalyst is of importance (Table S1). Nevertheless, the precise detrimental role of Cl⁻ ions is currently the subject of further investigation.

Notably, the optimal activity for catalysts prepared by using DP methodology was achieved at lower metal loadings, with 0.5 wt% Ir supported on CeO₂ and calcined at 200 °C (henceforth labelled 0.5Ir/CeO_{2(DP200C)}), leading to the best activity levels (Table 1, entry 6). Further improvement in catalytic activity could be achieved by varying the catalyst pre-treatment method. For instance, although 0.5Ir/CeO_{2(DP200C)} lead to a 33.4% yield of benzaldehyde in 3 h, the reduction (in H₂) of the same catalyst at 400 °C lead to a 54.8% yield of benzaldehyde in the same time (Figure 1 a). However, the performance

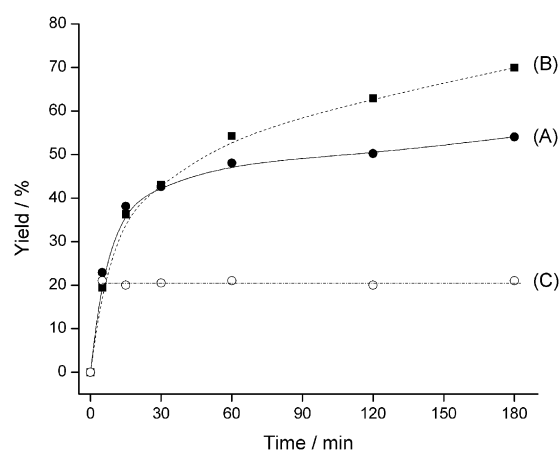


Figure 1. Temporal evolution of benzaldehyde with 0.5Ir/CeO_{2(DP400R)}: a) standard reaction; b) reaction performed with an added radical scavenger (1.0 mol% 2,6-di-*tert*-butyl-*p*-cresol); c) hot filtration experiment; the catalyst was removed from the hot reaction solution after 5 min. Further points represent the activity of the supernatant solution. Reaction conditions: 180 min, 90 °C, 0.2 M benzyl alcohol in toluene, 0.5 mol% Ir, 1 bar (100 kPa) O₂.

of this optimal catalyst is masked by a severe deactivation effect, which occurs after approximately 30 min of the reaction; as shown in Figure 1, the activity of this catalyst decreases significantly at a benzaldehyde yield of approximately 50%. In contrast, the less active catalysts, though possessing a lower reaction rate, did not suffer such extreme deactivation.

Nevertheless, the initial turnover frequency of this catalyst (0.5Ir/CeO_{2(DP400R)}) is more than three times higher than that achieved by the other pre-treated catalysts in the first 10 min of the reaction, which emphasises the beneficial effect of reductive pre-treatment on the activity of the catalyst. Although these TOFs are far lower than those previously observed for the solvent-free aerobic oxidation of benzyl alcohol with mono- and bimetallic Au, Pd and Au–Pd catalysts,^[19,10b] the re-

actions herein are performed in a solvent, at ambient pressures and in the absence of base and are similar in magnitude to those obtained for the aerobic oxidation with other precious metal-based catalysts under similar conditions (Figure 2).^[10c,14a]

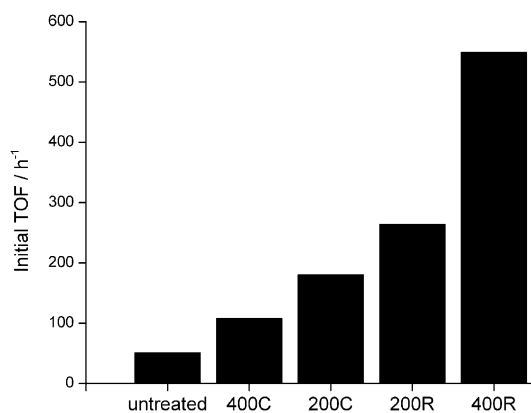


Figure 2. Initial turnover frequency observed for 0.5Ir/CeO₂ before and after various pre-treatment methods. Reaction conditions: 10 min, 90 °C, 0.2 M benzyl alcohol in toluene, 0.5 mol% Ir, 1 bar (100 kPa) O₂.

To rationalise the observed trend in reactivity, we subsequently investigated the pre-treated series of catalysts with a combination of spectroscopic and microscopic techniques. Because of the low Z-contrast of Ir and Ce, we were unable to determine any useful particle size and/or morphological data from the most active catalysts by using scanning TEM (Figure 3a and b). However, analysis of the 2.5Ir/MgO_(IMP200C) catalysts revealed that even though Ir was prepared through impregnation, it was present in nanoparticulate form, with most

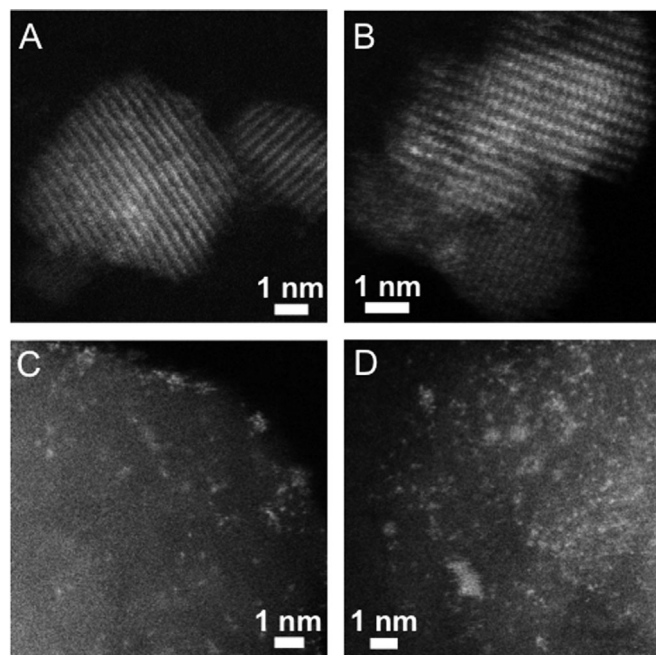


Figure 3. Scanning TEM analysis of 2.5Ir/CeO₂(IMP200C) (a,b) and 2.5Ir/MgO_(IMP200C) (c,d).

particles between 1 and 2 nm in size. Although this does not immediately confirm the nature of the Ir species in the CeO₂-supported materials, it suggests that Ir is nanoparticulate, especially given the more suitable preparation method used in that case (e.g. DP). Furthermore, the lack of any XRD reflections arising from Ir (not shown) suggests that any Ir species present in the material are below ± 10 nm in size, given the rough usability limit of the technique.

More insight regarding the nature of the Ir species in the active catalysts was, however, provided by various spectroscopic methods. Although UV/Vis analysis revealed little usable information, given the broad absorption arising from the CeO₂ support, Raman spectroscopy revealed that in addition to the main peak arising from CeO₂ (at 465 cm⁻¹), the as-synthesised and pre-treated catalysts had a weak broad signal at ± 550–600 cm⁻¹ (Figure S1). Such a signal has previously been attributed to Ir–O bonds,^[20] and its presence in all the materials suggests that Ir is not in metallic form. XPS analysis subsequently confirmed this, as no signal attributable to Ir⁰ was detected even after reduction at 400 °C. Instead, the XPS spectra of all samples consisted exclusively of Ir³⁺ and Ir⁴⁺ cations (Figures S2 and S3).

A linear correlation between the Ir³⁺/Ir⁴⁺ ratio and the initial turnover frequency of each catalyst is illustrated in Figure 4.

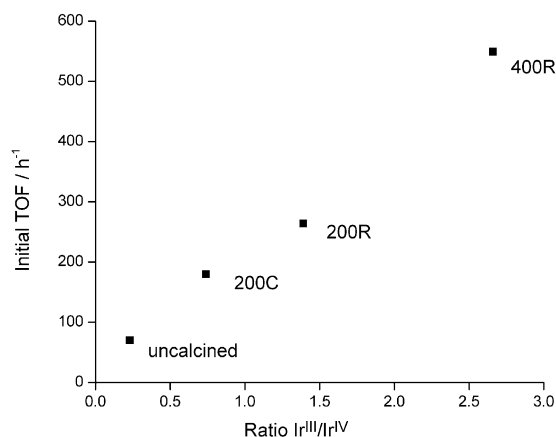


Figure 4. Straight line relationship observed between the initial turnover frequency and the Ir³⁺/Ir⁴⁺ ratio for 0.5Ir/CeO₂ after various pre-treatments. Reaction conditions: 10 min, 90 °C, 0.2 M benzyl alcohol in toluene, 0.5 mol% Ir. Reaction conditions: 180 min, 90 °C, 0.2 M benzyl alcohol in toluene, 0.5 mol% Ir, 1 bar (100 kPa) O₂.

This correlation suggests that Ir³⁺ is the key active component of the catalyst. The observation that the catalytic activity of the Ir-containing materials correlates so well with the fraction of Ir³⁺ appears to be unusual, because one would expect Ir⁴⁺ species to be the stronger oxidant for this reaction. However, Ir³⁺ species appear to be critical intermediates in homogeneous Ir chemistry, as Ir¹⁺–Ir³⁺ cycles are crucial for activity for transfer hydrogenations, hydroformylations and hydrogenations.^[4,13] Nevertheless, in the absence of direct mechanistic information of the reaction pathway mediated by these catalysts, it is difficult to conclude that the same chemistry is at play.

The presence of cationic Ir species and the presence of Ir–O bonds in the active catalysts suggest that the reactive species on the surface is nanoparticulate iridium oxide (Ir_xO_y). Given the oxidation states present, it is likely that IrO_2 (Ir^{4+}) and the sesquioxide Ir_2O_3 are the species present in the sample and that catalytic activity correlates with the fraction of Ir_2O_3 .

Notably, little Ce^{3+} was detected in any of the catalysts even after high-temperature reduction in H_2 . This is a crucial observation because Ce^{3+} is a critical component of various CeO_2 -supported Au catalysts for aerobic oxidation reactions, as it facilitates the formation of various metal hydroperoxy species, which can subsequently lead to catalytic activity.^[14b] Its absence in these highly active catalysts suggests that some alternative active species is formed in the present system.

Mechanistic investigations

We next turned our attention to the elucidation of the elementary reaction mechanism. We first excluded the possibility that the oxidative mechanism was radical based, as the addition of a known radical scavenger (2,6-di-*tert*-butyl-*p*-cresol, henceforth called ‘trap’) leads to no change in the initial rate of oxidation for 0.5 Ir/ $\text{CeO}_2(\text{DP400R})$ (Figure 1 b). We thus focused on the effect that substitution at the *para* position of benzyl alcohol had on the initial rate of activity (Hammett correlation). As illustrated in Figure 5, substitution at the *para* position of

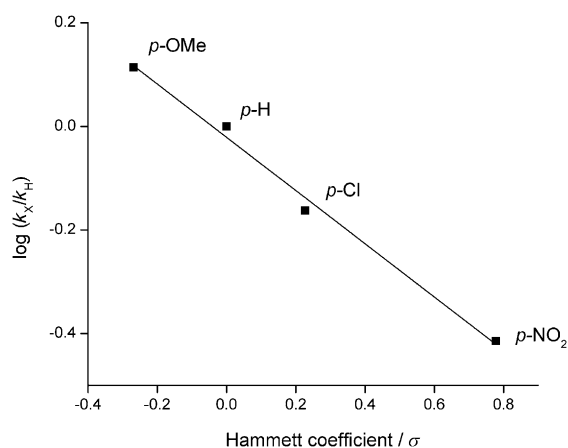


Figure 5. Hammett plot depicting the effect of the substitution of the *para* substituent of benzyl alcohol on the initial rate of oxidation. Reaction conditions: 180 min, 90 °C 0.2 M benzyl alcohol in toluene, 0.5 mol% Ir, 1 bar (100 kPa) O_2 .

benzyl alcohol leads to substantial modifications in the rate of reaction and a linear correlation ($R^2=0.993$) is observed between the logarithms of rate constants against the Hammett coefficient (σ) of each substituent (Hammett plot). The negative slope signifies that 1) the reaction rate is favoured by electron-donating substituents in the *para* position and 2) the transition state likely possesses cationic character. This immediately suggests that the cleavage of the benzylic C–H bond is rate determining, a hypothesis subsequently confirmed by examining the kinetic isotope effect (KIE) of the reaction. Monodeuter-

ation at the benzylic position lead to a 40–50% decrease in the reaction rate and KIE values of 1.88 at 90 °C and 1.75 at 70 °C (Figure S4). These relatively large KIE values confirm that the cleavage of the C–H bond and the subsequent formation of a transient carbocation is rate limiting. In addition, an Arrhenius expression was obtained from these experiments, which indicated that the reaction proceeded with an activation barrier of 55.0 kJ mol^{-1} and a pre-factor of $6.7 \times 10^7 \text{ s}^{-1}$, values that are in line with those of similar supported metal catalysts under comparable reaction conditions (Figure S5).^[10c,14a]

To gain further insight into the reaction mechanism, we determined the effect of the reactant concentrations on the initial rate of activity. These experiments demonstrate that although the reaction is first order in [benzyl alcohol] (Figure 6)

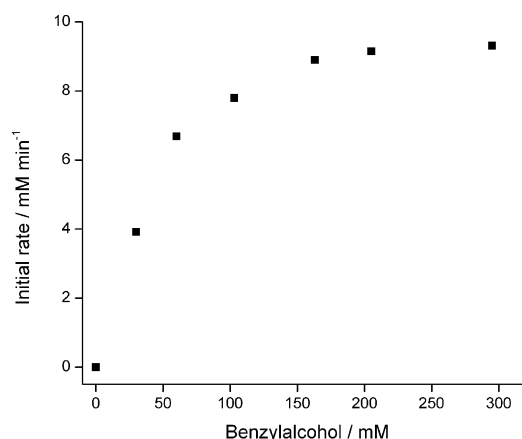


Figure 6. Effect of benzyl alcohol concentration on the initial rate of reaction for 0.5 Ir/ $\text{CeO}_2(\text{DP400R})$. Reaction conditions: 180 min, 90 °C, various concentrations of benzyl alcohol in toluene, 0.5 mol% Ir, 1 bar (100 kPa) O_2 .

and [catalyst] (Figure S6), it is zero order in $[\text{O}_2]$, at least at O_2 partial pressures of 0.2 bar and above (20 kPa; Figure 7). These observations are indicative of a reaction mechanism involving 1) the cleavage of the benzylic C–H bond by the catalyst,

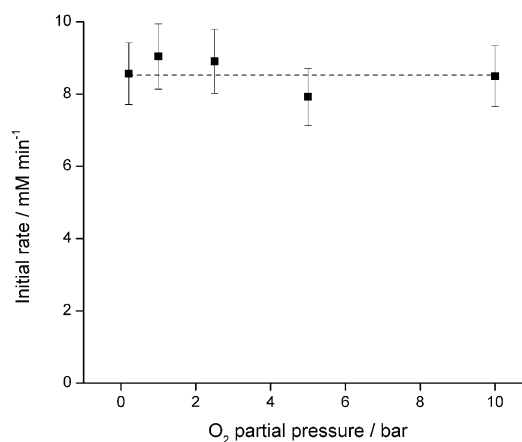
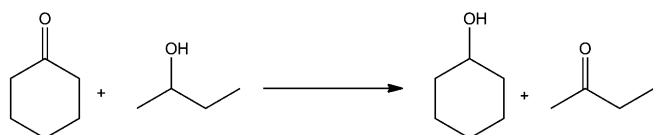


Figure 7. Effect of O_2 partial pressure on the initial rate of the reaction for 0.5 Ir/ $\text{CeO}_2(\text{DP400R})$. Reaction conditions: 180 min, 90 °C, 0.2 M benzyl alcohol in toluene, 0.5 mol% Ir.

which is rate determining and 2) a re-oxidation of the reduced metal centre, which is non-rate determining. The build-up of positive charge at the benzylic position signifies that the C–H cleavage occurs more quickly than the final formation of the C=O group. Such a mechanism would, however, require the formation of a metal hydride (M–H) or metal hydroxide (M–OH) intermediate, which would be formed via a β -hydride elimination of the adsorbed alcoholate and rupture of the C–H bond. Considering the probable nature of the active site (i.e. Ir_2O_3), it is likely that the intermediate species formed is Ir–OH, which is similar to the intermediates formed during Ru-catalysed aerobic oxidation.^[21] We emphasise that the ability of this catalyst to perform this oxidation with air at atmospheric pressure is highly promising, as it avoids issues associated with forming explosive mixtures of hydrocarbon vapours and O_2 and requires little technical expertise.

Notably, the concentration versus activity profile observed for benzyl alcohol is indicative of a Langmuir–Hinshelwood-type mechanism, in which the free alcohol is in equilibrium with the adsorbed, activated substrate, most likely an alcoholate-type species. Therefore, increasing the alcohol concentration beyond a certain level does not lead to an increase in the reaction rate, as the sites responsible for alcohol coordination and oxidation are fully saturated.

To determine 1) whether the mechanism proceeded via the dehydrogenation of the alcohol and subsequent re-oxidation of the reduced metal hydroxide intermediate with O_2 , or 2) whether adsorbed oxygen, either adsorbed direct by Ir_xO_y , or adsorbed and transported through CeO_2 , was responsible for the abstraction of the C–H hydride, we used the Meerwein–Ponndorf–Verley (MPV) transfer hydrogenation of cyclohexanone (Scheme 1), which as a useful probe reaction.



Scheme 1. Meerwein–Ponndorf–Verley reduction of cyclohexanone with 2-butanol. Reaction conditions: 60 min, 80 °C, 0.4 M cyclohexanone in 2-butanol, 0.5 mol% Ir.

Upon performing the MPV reaction in an inert atmosphere (nitrogen), quantitative conversion to cyclohexanol was achieved in short reaction times (Figure 8a). In contrast, upon performing the reaction in air, no cyclohexanol was observed (Figure 8c). The ability of the reaction to proceed in the absence of O_2 demonstrates that physisorbed oxygen is not responsible for the cleavage of the C–H bond. We thus propose that a typical dehydrogenation mechanism is in place, in which the metal hydroxide species, formed solely through the interaction of the alcohol and the catalyst, are subsequently re-oxidised by oxygen (in the case of aerobic oxidation) or by the unsaturated substrate (cyclohexanone, in the case of the MPV reaction). This agrees well with the zero-order dependence in O_2

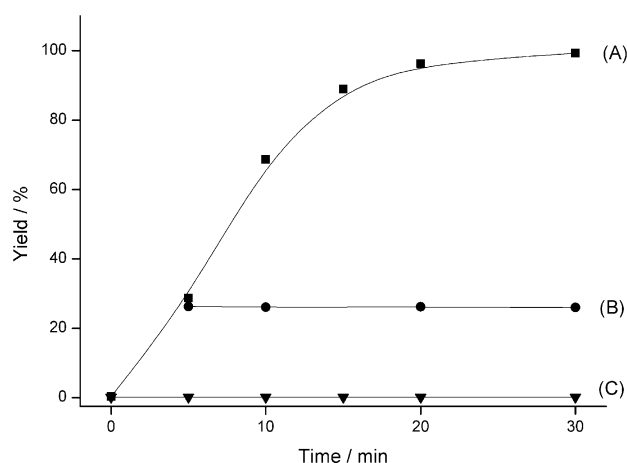


Figure 8. Temporal evolution of cyclohexanol by 0.5Ir/CeO₂(DP400R) under various conditions: a) standard reaction. Reaction conditions: 60 min, 80 °C, 0.4 M cyclohexanone in 2-butanol, 0.5 mol% Ir, N₂ atmosphere (1 bar; 100 kPa); b) hot filtration experiment. Catalyst removed after 5 min of the reaction; c) reaction performed in an O₂ atmosphere (1 bar; 100 kPa).

(Figure 7). A hot filtration experiment, in which the catalyst was removed at an intermediate stage of the reaction, confirmed that the MPV reaction is catalysed heterogeneously (Figure 8b).

Despite the negligible yield of cyclohexanol in an O₂ atmosphere (Figure 8c), some conversion of 2-butanol to 2-butanone was indeed observed. The lack of cyclohexanol yield in this reaction is due to the faster re-oxidation of the Ir–OH species by O₂ in comparison to a ketone; thus, the hydroxide species formed is removed from the catalyst surface before it reacts with cyclohexanone. Our observations during this reaction also provided some idea regarding the nature of the iridium oxide species on the catalyst surface; when the reaction was performed in an inert atmosphere (i.e. in which reaction is observed), the catalyst powder had a distinctive blue colour. In contrast, in an O₂ atmosphere, the powder was dark brown. Of the two oxides of Ir, iridium(III) oxide (Ir₂O₃) is blue and iridium(IV) oxide (IrO₂) is brown.

Catalyst deactivation

Our final series of investigations focused on the severe deactivation process observed for the most active alcohol oxidation catalyst 0.5Ir/CeO₂(DP400R) (Figure 1). We focused initially on the reuse of the catalyst to identify whether the catalyst was fully deactivated or whether the loss in activity observed was a feature of the reaction mechanism. However, the second use of a given charge of the catalyst leads to negligible levels of benzaldehyde formation, which suggests that the catalyst was deactivated. We therefore focused on the possible formation of minor quantities of benzoic acid, given the non-negligible loss in carbon balance during a reaction ($\pm 5\%$) and the known ability of carboxylic acids to poison various hydrogenation/oxidation catalysts. As shown in Figure 9, even by adding small amounts of benzoic acid to the initial reaction solution, a considerable decrease in activity is achieved, with the maximal

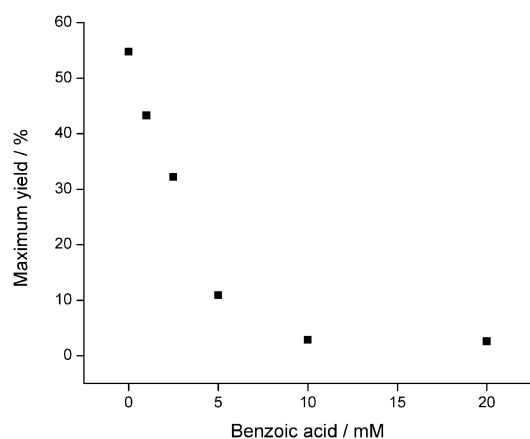


Figure 9. Effect of benzoic acid addition on the catalytic activity of 0.5Ir/CeO_{2(DP400R)}. Reaction conditions: 180 min, 90 °C, 0.2 M benzyl alcohol in toluene, 0.5 mol% Ir, 1 bar (100 kPa) O₂. Benzoic acid added at various initial concentrations.

yield of 0.5Ir/CeO_{2(DP400R)} decreasing to zero after the addition of only approximately 2.5 mol% of benzoic acid (relative to benzyl alcohol). However, even though benzoic acid was deliberately added to the reaction solution, it could not be detected by using GC–FID–MS. It is likely that once it is formed it quickly coordinates to the catalyst surface and thus inhibits the coordination and subsequent reaction of the alcohol substrate.

To rationalise the formation of benzoic acid, we reasoned that the over-oxidation of benzaldehyde to benzoic acid could proceed via free-radical intermediates. Given the positive effect of the addition of the radical trap in terms of both catalyst deactivation and carbon balance (Figure 1 b), it seems highly likely that benzoic acid forms through the free-radical (auto)oxidation of benzaldehyde,^[22] given that the addition of a known radical scavenger minimises deactivation and leads to carbon balance of ± 100%. By adding only 1 mol% of trap (relative to the starting benzyl alcohol concentration), a 25% increase in benzaldehyde yield can be achieved, which demonstrates the effect of oxygen-centred radicals on mediating the formation of benzoic acid and causing catalyst deactivation. It is likely that this deactivation through acid formation is the reason why many investigations concerning alcohol oxidation with (noble) metal-based catalysts are performed in a basic medium; although leading to the formation of the corresponding carboxylic acid through hemiacetal formation, neutralisation of the acid through formation of the sodium adduct removes its coordinative ability, thus freeing the metal from the undesired carboxylate coordination. Upon treating the deactivated catalyst with a dilute solution of NaOH (0.1 M, 20 mL g⁻¹ of the catalyst), full catalyst activity was restored (Figure 10).

XPS analysis demonstrated that the spent catalyst, that is 0.5Ir/CeO_{2(DP400R)} after the reaction, had a significantly lower fraction of Ir³⁺. Given that Ir³⁺ is the critical component of the catalyst (see above), the formation of Ir⁴⁺ during the reaction could also contribute to catalyst deactivation. Nevertheless, it is impossible to confirm at this stage whether the formation of Ir⁴⁺ precedes the formation of carboxylic acid (i.e. whether the oxidation of Ir³⁺ to Ir⁴⁺ is responsible for the formation of car-

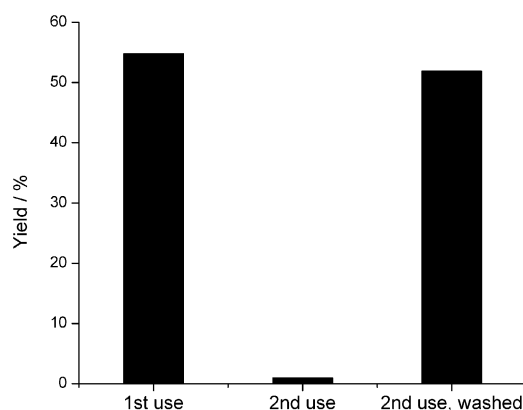


Figure 10. Reuse ability of 0.5Ir/CeO_{2(DP400R)} without and with an NaOH washing method. Reaction conditions: 180 min, 90 °C, 0.2 M benzyl alcohol in toluene, 0.5 mol% Ir, 1 bar (100 kPa) O₂.

boxylic acid), whether this undesirable increase in oxidation state is due to the formation of carboxylic acid or whether the two features are independent of one another.

Conclusions

We have shown that by supporting iridium on CeO₂, a highly active and selective heterogeneous catalyst for various transfer hydrogenations (aerobic alcohol oxidation and Meerwein–Ponndorf–Verley hydrogenation) can be prepared. The activity of this catalyst is related both to the properties of the support, that is the ability of CeO₂ to transport oxygen, and the iridium oxide centre. Key spectroscopic and catalytic investigations suggest that the major active species is nanoparticulate Ir₂O₃, which are preferentially formed through the high-temperature (400 °C) reduction of the as-prepared catalyst.

The kinetic parameters and mechanistic features of this system are consistent with a β-hydride elimination mechanism and indicate that the ability of this catalyst to mediate 1) the aerobic oxidation of alcohols and 2) the Meerwein–Ponndorf–Verley transfer hydrogenation of ketones is related to its ability to form metal hydroxide species, which are subsequently transferred to either a molecular oxygen or a ketone, respectively. We emphasise that this catalyst can perform these reactions at mild temperatures (< 100 °C) in the absence of stoichiometric quantities of a base (i.e. base-free) and with a molecular oxygen or air at ambient pressure. Finally, we have demonstrated that the catalyst suffers from a severe deactivation process, which is caused by the radical-based byproduct of benzoic acid. The coordination of the carboxylate to the metal oxide centre significantly decreases its activity for this reaction, though this can be limited by adding trace quantities of a radical scavenger to the initial reaction solution.

We anticipate that the ability of this catalyst to mediate these transformations will open the possibility of further developing heterogeneous iridium-based catalysts for a number of other crucial transformations, such as hydrogenation, hydroformylation and C–H activation.

Experimental Section

Catalyst synthesis

Various metal oxide-supported Ir catalysts were prepared through the wet impregnation of the relevant metal oxide by an appropriate amount of aqueous solution of hexachloroiridic acid (H_2IrCl_6 , $3.7 \text{ mg}_l \text{ mL}^{-1}$). The solvent was evaporated at 90°C and the resultant paste dried in an oven at 110°C for 16 h. Analogous materials were also prepared by using a DP methodology. In this case, an aqueous solution containing the appropriate amount of CeO_2 and H_2IrCl_6 was stirred at RT. The pH was subsequently raised to 10 with NaOH (0.1 M), and the solution was stirred for 24 h at ambient temperature. The solid catalyst was filtered under vacuum, and the catalyst was washed thoroughly with distilled water (2 L g^{-1} of catalyst) before drying in an oven at 110°C for 16 h. The dried catalysts were subsequently pre-treated in a sealed combustion furnace in a flow of air (for calcination) or H_2 (for reduction) for 3 h at the required temperature described in the text (ramp rate: $20^\circ\text{C min}^{-1}$).

Catalyst characterisation

The as-synthesised and pre-treated catalysts were characterised by using a combination of scanning TEM, XRD, XPS and Raman spectroscopy techniques. XPS analysis was performed by using a PHI 5000 VersaProbe spectrometer (ULVAC-PHI, Inc.) equipped with a 180°C spherical capacitor energy analyser and a multi-channel detection system with 16 channels. The XPS spectra were acquired at a base pressure of $5 \times 10^{-8} \text{ Pa}$ by using a focused scanning monochromatic AlK_{α} source (1486.6 eV) with a spot size of $200 \mu\text{m}$. The instrument was run in the FAT analyser mode, with electrons emitted at 45° to the surface normal. Pass energy used was 187.85 eV for survey scans and 46.95 eV for detailed spectra. Charge neutralisation was applied throughout the analysis by using both a cool cathode electron flood source (1.2 eV) and low-energy Ar^+ ions (10 eV). Data were analysed with CasaXPS software. Powder XRD was performed by a PANalytical X'Pert PRO X-ray diffractometer equipped with a CuK_{α} radiation source (40 kV and 40 mA) and a Ni filter. Raman spectra were recorded by using a Renishaw's InVia Raman microscope. Samples were irradiated with the 514.5 nm line of an Ar-ion laser at 20 mW power.

Catalyst testing

The aerobic oxidation of benzyl alcohol was performed in a 50 mL round bottom flask sealed with a balloon of O_2 or air. The reactor contained the desired amount of the catalyst (typically corresponding to 0.5 mol% Ir) and the reactant solution (0.2 M benzyl alcohol in toluene; total volume: 5 mL). Reactions were performed between 70 and 110°C , but typically at 90°C for 3 h. High-pressure experiments were performed in a Parr autoclave reactor (100 mL) lined with Teflon (working volume: 70 mL). Product analysis and quantification was performed by using GC-FID analysis (30 m FFAP column) using a biphenyl internal standard. The MPV transfer hydrogenation of cyclohexanone was also performed in a 50 mL round bottom flask equipped with a reflux condenser and kept under a N_2 atmosphere. The vessel was charged with the reactant solution (0.4 M cyclohexanone in 2-butanol) and the appropriate amount of the catalyst (corresponding to 0.5 mol% Ir). Reactions were performed at 80°C and quantified against a biphenyl internal standard by using GC-FID analysis (30 m FFAP column).

Acknowledgements

We acknowledge ETH Zurich for financial support (project ETH-17 09-3) and are indebted to Dr. Frank Krumeich for the TEM measurements.

Keywords: elimination • heterogeneous catalysis • iridium • oxidation • hydrogenation

- [1] a) M. S. Sanford, J. A. Love, R. H. Grubbs, *J. Am. Chem. Soc.* **2001**, *123*, 6543–6554; b) T. M. Trnka, R. H. Grubbs, *Acc. Chem. Res.* **2001**, *34*, 18–29; c) R. H. Grubbs, S. Chang, *Tetrahedron* **1998**, *54*, 4413–4450; d) E. L. Dias, S. T. Nguyen, R. H. Grubbs, *J. Am. Chem. Soc.* **1997**, *119*, 3887–3897; e) A. Fürstner, *Angew. Chem.* **2000**, *112*, 3140–3172; *Angew. Chem. Int. Ed.* **2000**, *39*, 3012–3043.
- [2] a) N. Miyaura, A. Suzuki, *Chem. Rev.* **1995**, *95*, 2457–2483; b) N. Miyaura, T. Yanagi, A. Suzuki, *Synth. Commun.* **1981**, *11*, 513–519.
- [3] a) N. F. Gol'dshleger, V. V. Es'kova, A. E. Shilov, A. A. Shteinman, *Russ. J. Phys. Chem.* **1972**, *46*, 785; b) R. A. Periana, D. J. Taube, S. Gamble, H. Taube, T. Satoh, H. Fujii, *Science* **1998**, *280*, 560–564; c) C. Hammond, S. Conrad, I. Hermans, *ChemSusChem* **2012**, *5*, 1668–1686.
- [4] a) J. Choi, A. H. R. MacArthur, M. Brookhart, A. S. Goldman, *Chem. Rev.* **2011**, *111*, 1761–1779; b) I. Göttker-Schnetmann, P. White, M. Brookhart, *J. Am. Chem. Soc.* **2004**, *126*, 1804–1811; c) R. H. Crabtree, M. F. Mellea, J. M. Mihelcic, J. M. Quirk, *J. Am. Chem. Soc.* **1982**, *104*, 107–113; d) R. Crabtree, *Acc. Chem. Res.* **1979**, *12*, 331–338; e) R. Ahuja, B. Punji, M. Findlater, C. Supplee, W. Schinski, M. Brookhart, A. S. Goldman, *Nat. Chem.* **2011**, *3*, 167–171; f) R. Kawahara, K.-i. Fujita, R. Yamaguchi, *J. Am. Chem. Soc.* **2012**, *134*, 3643–3646; g) C. Cheng, M. Brookhart, *J. Am. Chem. Soc.* **2012**, *134*, 11304–11307; h) S. Park, D. Bezier, M. Brookhart, *J. Am. Chem. Soc.* **2012**, *134*, 11404–11407.
- [5] a) B. A. Arndtsen, R. G. Bergman, *Science* **1995**, *270*, 1970–1973; A. M. Voutchkova, R. H. Crabtree, *J. Mol. Catal. A* **2009**, *312*, 1–6; b) J. Y. Cho, M. K. Tse, D. Holmes, R. E. Maleczka, M. R. Smith, *Science* **2002**, *295*, 305–308; c) J. K. Hoyano, A. D. McMaster, W. A. G. Graham, *J. Am. Chem. Soc.* **1983**, *105*, 7190–7191.
- [6] a) J. Lin, B. Qiao, J. Liu, Y. Huang, A. Wang, L. Li, W. Zhang, L. F. Allard, X. Wang, T. Zhang, *Angew. Chem.* **2012**, *124*, 2974–2978; *Angew. Chem. Int. Ed.* **2012**, *51*, 2920–2924; b) F. Morfin, S. Nassreddine, J. L. Rousset, L. Piccolo, *ACS Catal.* **2012**, *2*, 2161–2168; c) L. Piccolo, S. Nassreddine, F. Morfin, *Catal. Today* **2012**, *189*, 42–48.
- [7] a) W. Cai, F. Wang, C. Daniel, A. C. van Veen, Y. Schuurman, C. Descorme, H. Provendier, W. Shen, C. Mirodatos, *J. Catal.* **2012**, *286*, 137–152; b) F. Wang, W. Cai, H. Provendier, Y. Schuurman, C. Descorme, C. Mirodatos, W. Shen, *Int. J. Hydrogen Energy* **2011**, *36*, 13566–13574; c) W. Du, Q. Wang, D. Saxner, N. A. Deskins, D. Su, J. E. Krzanowski, A. I. Frenkel, X. Teng, *J. Am. Chem. Soc.* **2011**, *133*, 15172–15183.
- [8] a) J. F. Hull, D. Balcells, J. D. Blakemore, C. D. Incarvito, O. Eisenstein, G. W. Brudvig, R. H. Crabtree, *J. Am. Chem. Soc.* **2009**, *131*, 8730–8733; b) D. B. Grotjahn, D. B. Brown, J. K. Martin, D. C. Marelus, M.-C. Abadjian, H. N. Tran, G. Kalyuzhny, K. S. Vecchio, Z. G. Specht, S. A. Cortes-Llomas, V. Miranda-Soto, C. van Niekerk, C. E. Moore, A. L. Rheingold, *J. Am. Chem. Soc.* **2011**, *133*, 19024–19027.
- [9] a) H. Shi, O. Y. Gutierrez, G. L. Haller, D. Mei, R. Rousseau, J. A. Lercher, *J. Catal.* **2013**, *297*, 70–78; b) H. Shi, X. Li, G. L. Haller, O. Y. Gutierrez, J. A. Lercher, *J. Catal.* **2012**, *295*, 133–145; c) J. Moran, A. Preetz, R. A. Mesch, M. J. Krische, *Nat. Chem.* **2011**, *3*, 287–290; d) I. Piras, R. Jennerjahn, R. Jackstell, A. Spannenberg, R. Franke, M. Beller, *Angew. Chem.* **2011**, *123*, 294–298; *Angew. Chem. Int. Ed.* **2011**, *50*, 280–284.
- [10] a) A. S. K. Hashmi, G. J. Hutchings, *Angew. Chem.* **2006**, *118*, 8064–8105; *Angew. Chem. Int. Ed.* **2006**, *45*, 7896–7936; b) K. Mori, T. Hara, T. Mizugaki, K. Ebitani, K. Kaneda, *J. Am. Chem. Soc.* **2004**, *126*, 10657–10666; c) K. Yamaguchi, N. Mizuno, *Angew. Chem.* **2002**, *114*, 4720–4724; *Angew. Chem. Int. Ed.* **2002**, *41*, 4538–4540.
- [11] a) M. Sankar, N. Dimitratos, P. J. Miedziak, P. P. Wells, C. J. Kiely, G. J. Hutchings, *Chem. Soc. Rev.* **2012**, *41*, 8099–8139; b) D. M. Alonso, S. G. Wettstein, J. A. Dumesic, *Chem. Soc. Rev.* **2012**, *41*, 8075–8098; c) J. A. Lopez-Sanchez, N. Dimitratos, N. Glanville, L. Kesavan, C. Hammond,

- J. K. Edwards, A. F. Carley, C. J. Kiely, G. J. Hutchings, *Appl. Catal. A* **2011**, *391*, 400–406.
- [12] a) F. Cavani, N. Ballarini, S. Luciani, *Top. Catal.* **2009**, *52*, 935–947; b) F. Cavani, J. H. Teles, *ChemSusChem* **2009**, *2*, 508–534; c) R. A. Sheldon, *Chem. Commun.* **2008**, 3352–3365.
- [13] T. Suzuki, *Chem. Rev.* **2011**, *111*, 1825–1845.
- [14] a) A. Abad, A. Corma, H. Garcia, *Chem. Eur. J.* **2008**, *14*, 212–222; b) A. Abad, P. Concepcion, A. Corma, H. Garcia, *Angew. Chem.* **2005**, *117*, 4134–4137; *Angew. Chem. Int. Ed.* **2005**, *44*, 4066–4069.
- [15] a) F. Moreau, G. C. Bond, A. O. Taylor, *J. Catal.* **2005**, *231*, 105–114; b) F. Moreau, G. C. Bond, A. O. Taylor, *Chem. Commun.* **2004**, 1642–1643.
- [16] F. Moreau, G. C. Bond, *Catal. Today* **2006**, *114*, 362–368.
- [17] H.-S. Oh, J. H. Yang, C. K. Costello, Y. M. Wang, S. R. Bare, H. H. Kung, M. C. Kung, *J. Catal.* **2002**, *210*, 375–386.
- [18] Y. Huang, A. Wang, L. Li, X. Wang, T. Zhang, *Catal. Commun.* **2010**, *11*, 1090–1093.
- [19] D. I. Enache, J. K. Edwards, P. Landon, B. Solsona-Espriu, A. F. Carley, A. A. Herzing, M. Watanabe, C. J. Kiely, D. W. Knight, G. J. Hutchings, *Science* **2006**, *311*, 362–365.
- [20] a) Y. B. Mo, I. C. Stefan, W. B. Cai, J. Dong, P. Carey, D. A. Scherson, *J. Phys. Chem. B* **2002**, *106*, 3681–3686; b) R. K. Kowar, P. S. Chigare, P. S. Patil, *Appl. Surf. Sci.* **2003**, *206*, 90–101.
- [21] a) N. Mizuno, K. Yamaguchi, *Catal. Today* **2008**, *132*, 18–26; b) K. Yamaguchi, N. Mizuno, *Chem. Eur. J.* **2003**, *9*, 4353–4361.
- [22] I. Hermans, J. Peeters, L. Vereecken, P. A. Jacobs, *ChemPhysChem* **2007**, *8*, 2678–2688.

Received: April 4, 2013

Published online on ■ ■ ■ ■, 0000